

MACIEJ J. MENDECKI*[#], KRZYSZTOF JOCHYMCZYK*,
WACŁAW M. ZUBEREK*, RADOSŁAWA TOMASZEWSKA*

**DETERMINATION OF ELASTIC PARAMETERS OF NEAR-SURFACE LAYERS
OVER SUBSIDENCE TROUGH DEVELOPMENT DURING
LONGWALL EXPLOITATION**

**WYZNACZENIE PARAMETRÓW SPRĘŻYSTYCH PŁYTKIEGO OŚRODKA GEOLOGICZNEGO
NAD WYKSZTAŁCAJĄCĄ SIĘ NIECKĄ OBNIŻENIOWĄ**

Seismic and geodetic studies were carried out before, during, and after underground exploitation of a coal bed in Katowice – Kleofas Coal Mine, located in the Upper Silesia Coal Basin, Poland. Development of a subsidence trough was completed approximately 3 months after passage of a longwall exploitation in the coal seam. This was the time required for the subsidence trough to appear on the surface, which was confirmed by levelling measurements. Sharp changes in the elastic parameters were observed on each profile during subsidence trough development. This observation can result from changing tension and compression forces caused by increase and/or decrease of the elastic parameters of the rock mass. After completion of subsidence trough development, the rock mass appeared to return to its isotropic state and the observed changes ceased. Some minor fluctuations were noted, but they probably resulted from changes in groundwater levels, which might have affected the measured parameters.

Keywords: shallow seismics, wave velocity anisotropy, shear modulus, attenuation, subsidence trough, underground coal mining.

Podziemna eksploatacja górnicza wywołuje niebezpieczne deformacje powierzchni terenu. W rejonie prowadzonej ścianowej eksploatacji górnicznej przez KWK Katowice – Kleofas wykonano dwuletnie, cykliczne pomiary sejsmiczne oraz geodezyjne. Największe wartości składowych pionowych przemieszczeń punktów osnowy geodezyjnej zaobserwowano 3 miesiące po przejściu frontu eksploatacji ścianowej w pokładzie węgla kamiennego na głębokości ponad 600 metrów poniżej poziomu terenu. Podczas procesu wykształcania się niecki obniżeniowej stwierdzono występowanie gwałtownych zmian parametrów sprężystych płytkiego ośrodka geologicznego. Zmiana tych parametrów wynika ze zmiennego w czasie stanu naprężeń ściskających i rozciągających w skałach. Po zakończeniu procesu wykształcania się niecki obniżeniowej mierzone parametry generalnie ustabilizowały się, co świadczy o powrocie środowiska

* FACULTY OF EARTH SCIENCES, UNIVERSITY OF SILESIA, 60 BEDZINSKA STR., 41-200 SOSNOWIEC, POLAND

Corresponding author: maciej.mendecki@us.edu.pl

geologicznego do stanu izotropowego. Występujące wtedy niewielkie wahania parametrów wynikają ze zmiany poziomu zwierciadła wody.

Słowa kluczowe: płytka sejsmika, anizotropia prędkości fal sejsmicznych, moduł ścinania, tłumienie fal sejsmicznych, niecka obniżeniowa, eksploatacja węgla kamiennego

1. Introduction

Underground mining exploitation has a large influence on the surface of the Earth. Exploitation impacts are particularly important in urban areas (Jochymczyk, 2005; Bogusz & Mendecki, 2011). Surface subsidence above the underground mining, especially coal mining, represents one of the most negative influences of mining and is well known and recognized, *inter alia*, in the Upper Silesia Coal Basin. In this area, extensive underground coal mining has been carried out for several dozen years and huge amounts of coal have been extracted (Gustkiewicz et al., 2002). Geodetic monitoring of the subsidence trough development is widely applied in the mining areas using GPS, levelling, and total station techniques (e.g.: Jochymczyk, 2005; Blachowski et al., 2009; Doležalová et al., 2009; Bogusz & Mendecki, 2011; Doležalová et al., 2012; Kajzar & Doležalová, 2013; Kadlečík et al., 2015). In recent years, InSAR and PsInSAR studies have also been very popular (e.g., Kadlečík et al., 2010; Mirek & Mirek, 2016; Karakostas et al., 2017).

Subsidence trough development (Fig. 1) is not just a simple deformation of the surface. The Knothe-Budryk theory, which was developed in the 1950s by Knothe and Budryk, describes among others the course of deformation occurring on the surface, caused by mining (Kochmański, 1980; Knothe 1980, 1984). According to the theory, there are several areas with different stress orientations (tension and compression) in a subsidence trough, which impacts changes of velocity, attenuation, and stress moduli (Gustkiewicz et al., 2002; Jochymczyk, 2005). Moreover, this process differentiates in time and is strongly dependent on local geologic structure.

Therefore, the main aim of this study was to observe the dynamic elastic properties of the subsurface brittle and ductile layers during subsidence trough development. In order to perform this research, the traditional and modern seismic methods, shallow seismic refraction travel-times approach (SR) and multichannel analysis of surface waves (MASW), were applied. The goal was achieved by regular time-lapse seismic and levelling measurements carried out on the surface over the underground operating longwall. The seismic profiles were formed into a rosette with the 45° angle between each survey branch. Levelling measurements allowed the calculation of temporal subsidence for each bench mark.

Seismic methods were used to evaluate the elastic parameter values such as velocity (longitudinal wave, V_p , and shear wave, V_s), elastic moduli (e.g., shear modulus) and attenuation coefficient as well as the depth of the distinguished geophysical layers. The seismic profiles formed in a rosette allowed the observation of temporal and spatial changes to the parameters mentioned above. Seismic measurements are frequently applied to calculate the velocity anisotropy in rocks, especially in those occurring in quarries, which allows the estimation of rock quality (Bamford & Nunn, 1979; Crampin et al., 1980; Carvalho et al., 2000; Jochymczyk, 2005; Stan-Kleczek & Mendecki, 2014; Stan-Kleczek & Mendecki, 2016).

Subsidence trough parameters are described by the measurement of horizontal u and vertical ε components of displacement and maximum subsidence w_{max} . Figure 1 shows spatial distributions of deformation in the surface area over the exploited inclined coal seam. The stress state is variable in time during the exploitation process (Knothe, 1984). The form of the surface deformation

is strongly affected by previous exploitation. In the study area, mining was carried out during the last century in dozens of seams. The total thickness of exploited seams reached over 20 m and caused a complicated distribution of stress in the rock mass. Observed on the surface, the stress-strain relationship has anisotropic behavior and depends on the direction of the longwall exploitation and local geology.

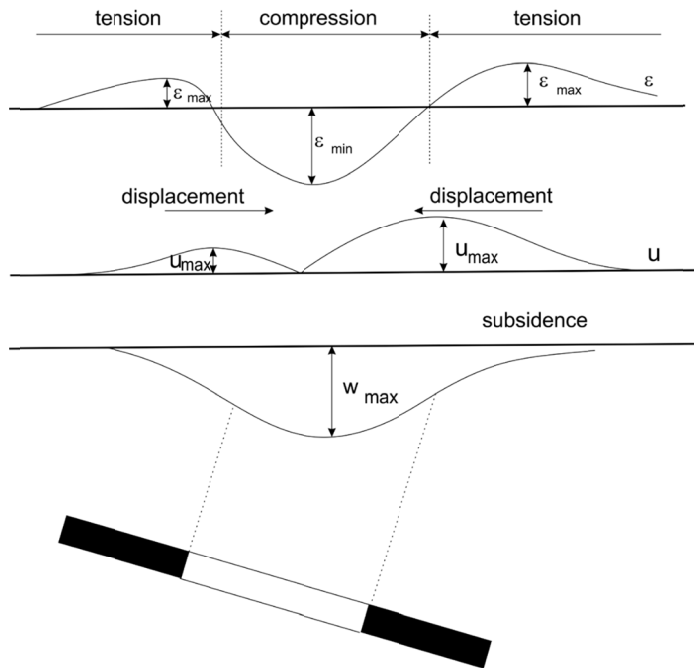


Fig. 1. Subsidence trough development and rock mass deformation due to longwall exploitation. The top scheme represents the strain changes, ϵ , in the middle scheme the ground displacements u are shown, and the bottom figure shows the subsidence development over the sloping coal seam (Knothe, 1980; Kochmański, 1980)

2. Site characterization

The study area was located in the Upper Silesia Coal Basin (UBSC), within the Main Anticline, in the subarea of the City of Katowice. The mining exploitation of the Katowice-Kleofas Coal Mine was conducted in several coal seams: 402, 404/5, 405, 407/4, 412, 416, 501, 504 and 510 at a depth of about 140 m up to 700 m below the surface. During the seismic surveys the mining exploitation with caving was carried out in two parallel longwalls: No. 201 (225 m \times 1300 m) and No. 202 (225 m \times 225 m) in the 510 coal seam at a depth of about 700 m below surface. The extracted coal layer was about 2 m high. The location of the longwalls, seismic rosette, and bench marks was presented in Fig. 2 – left map.

The local geologic conditions were identified via the P-2 (Fig. 2-right) borehole located in the vicinity of the rosette (Fig. 2-left map). A ductile layer is located from the surface of the ground to a depth of about 4 meters which overlays the Carboniferous brittle layer. The ductile

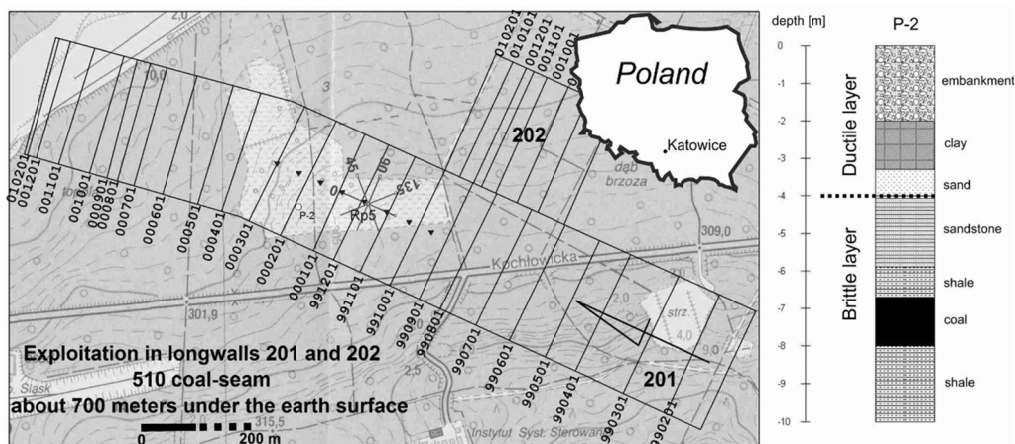


Fig. 2. Location of the seismic survey profiles forming the rosette and levelling bench marks on the background of mining exploitation, location of the P-2 borehole (left map) and its geological profile (right)

layer consists of anthropogenic material, clay, and sand. The brittle layer is composed of sandstone and shale with a small coal seam. This brittle complex is very heavily cracked and fissured into centimeter-sized cubes (Fig. 2-right).

3. Methodology

3.1. Levelling measurements

The underground exploitation disturbs rock mass equilibrium and results in changes (in time and space) to the state of stress. Rock mass deformation processes, resulting from the mine operation, can be observed using geodetic (levelling, tachymetry, GPS) and geophysical (seismic, geoelectrical, electromagnetic) methods. The advantage of geophysical methods is the ability to study the physical parameters of the rock at different depths during the deformation process. Moreover, the seismic methods can examine the subsidence development process that caused variations in velocity and/or attenuation of seismic waves in different directions. The levelling measurements enable the calculation of the bench mark subsidence with an accuracy of 2 mm/km. Levelling data were plotted as subsidence against time in order to determine the average time of the Maximum Surface Subsidence Velocity (MSSV). The applied model of subsidence was as follows (Bogusz & Mendecki, 2011):

$$h(t) = a_1 \left[1 - \left(e^{\frac{t-a_2}{a_3}} + 1 \right)^{-1} \right] \quad (1)$$

where: $h(t)$ – subsidence in meters, t – time in days, a_1 – maximum subsidence with time tends to infinity, a_2 – MSSV average time, a_3 – curvature factor.

The presented function (1) is similar in shape to functions applied in mining geodesy to describe surface subsidence over time (e.g., Knothe, 1980; Kochmański, 1980). The a_1 parameter corresponds with final subsidence in infinity time (Bogusz & Mendecki, 2011), the a_3 parameter is related to the c parameter (Knothe; 1980, Kochmański, 1980). Moreover, a_2 is the MSSV average time (Bogusz & Mendecki, 2011). The surface subsidence velocity as a time differential is calculated as follows (Bogusz & Mendecki, 2011):

$$v(t) = \frac{dh(t)}{dt} = \frac{a_1}{a_3} \exp\left(\frac{t-a_2}{a_3}\right) \cdot \left(\exp\left(\frac{t-a_2}{a_3}\right) + 1\right)^{-2} \quad (2)$$

Equation (2) represents the analytical form of the velocity distribution during the subsidence process, which is characterized by a bell-shaped curve. The maximum of the velocity distribution corresponds to the highest velocities of the subsidence process observed for the given benchmark.

3.2. Seismics

Seismic refraction is a widely used technique to recognize shallow geology, especially elastic parameters of near-surface layers (e.g., Belfer et al., 1998; Turesson, 2007; Carvalho et al., 2009; Sloan et al., 2013). This method allows evaluation of apparent P-wave velocities and the thickness of distinguished layers. Other parameters, such as S-wave velocity, were obtained using MASW technique, which has become a popular tool for shallow site characterization. However, its limitations must always be considered (e.g., Park et al., 1999; Lin et al., 2004; Xu & Butt, 2006; Foti et al., 2014; Ismail et al., 2014; Stan-Kłeczek & Mendecki, 2014; Dal Moro et al., 2015a; Dal Moro et al., 2015b).

Shallow Seismic Refraction and MASW methods were applied to analyze 37 measurements to investigate spatial and temporal changes of elastic parameters in subsurface layers during extraction of the coal bed over 2 years of observations. The seismic measurements were performed using the 12 channels Terraloc Mk6 apparatus connected with 10 Hz geophones at 0.5 ms sampling intervals. A total of 5 survey profiles, with 4 m geophones spacing, were formed into a rosette with arms arranged at a 45° angle to each other. The source for the P-wave survey was a 10-kg sledge hammer on a steel-plate. The field methodology for both techniques is similar; therefore, the same data sets were applied to analyze both results, and one seismic trace (with the 4 m offset) was always chosen for MASW processing.

Apparent P-wave velocity was calculated from picked P-wave arrivals. The seismic traces were analyzed in order to obtain travel-time graphs and, subsequently, the velocities of the first and second layer were estimated from the $x - t$ slopes and the ductile layer depth was calculated from intercept time. The MASW data interpretation was executed in winMASW software using the genetic algorithms to invert the observed Rayleigh dispersion curve into S-wave velocity vertical profiles (Dal Moro et al., 2007). In addition, the inversion allowed determination of parameters such as density, thickness, shear modulus.

Determination of the attenuation coefficient of seismic waves is a more difficult task and susceptible to higher error. The wave attenuation coefficient can be defined as a wave amplitude decrease over distance from the source (Schön, 1996):

$$A(x) = A(x_0) \left(\frac{x_0}{x} \right)^n \exp[-\alpha(x - x_0)] \quad (3)$$

where: $A(x_0)$ – wave amplitude in a source, α – attenuation coefficient, $\exp[-\alpha(x - x_0)]$ – wave amplitude decrease caused by attenuation, $\left(\frac{x_0}{x} \right)^n$ – factor characterizing a geometric expansion of a wave front.

4. Results and discussion

The presented results are an attempt to collate levelling measurements such as displacement and subsidence velocity changes with the P- and S-wave velocity, shear modulus, and attenuation coefficient variations in time and space.

4.1. Levelling Measurements

The subsidence trough development was observed by time-lapse measurements performed on 8 benchmarks (Fig. 2-left). The center of the seismic rosette coincided with the 5th benchmark. The levelling measurements are shown in Fig. 3 (black dots), where the horizontal axis is in the time domain and two vertical axes represent subsidence in meters and subsidence velocity in meters per day respectively.

Analysis of subsidence allows us to distinguish, overlapping with different subsidence rates, two modes of the subsidence process. The first one is observed as a steep rapid collapse of the ground over time and the second as a gentle and slow subsidence having a rate visibly different than the initial one. The least-squares technique was applied to produce two subsidence modes according to equation (1). Results of the estimation, consisting of mode parameters and determination coefficient R^2 , were compared in Table 1. In Fig. 3, a black solid line represents the first model and a black dashed line is the second model.

Because the subsidence modes were separately identified, the velocity distribution could also be calculated and plotted as a bell-shape curve in Fig. 3, where the gray solid line represents the first mode and a gray dashed line represents the second mode. We assume that the distinguished subsidence modes are related to the deformation of the selected brittle and ductile layers from the geological profile (Fig. 2).

Parameter a_2 corresponds to the middle time of the maximum surface subsidence velocity. The values obtained, 146 day and 267 days, are indicated on dates of maximum velocity of subsidence: 2000-01-25 and 2000-05-26, respectively, and seem acceptable with the observed subsidence curve.

TABLE 1

Calculated subsidence mode parameters

Model	Mode parameters			R^2
	a_1 [m]	a_2 [days]	a_3 [days]	
first collapse	-0.729	145.96	30.75	0.9983
second collapse	-1.508	267.11	174.27	0.9977

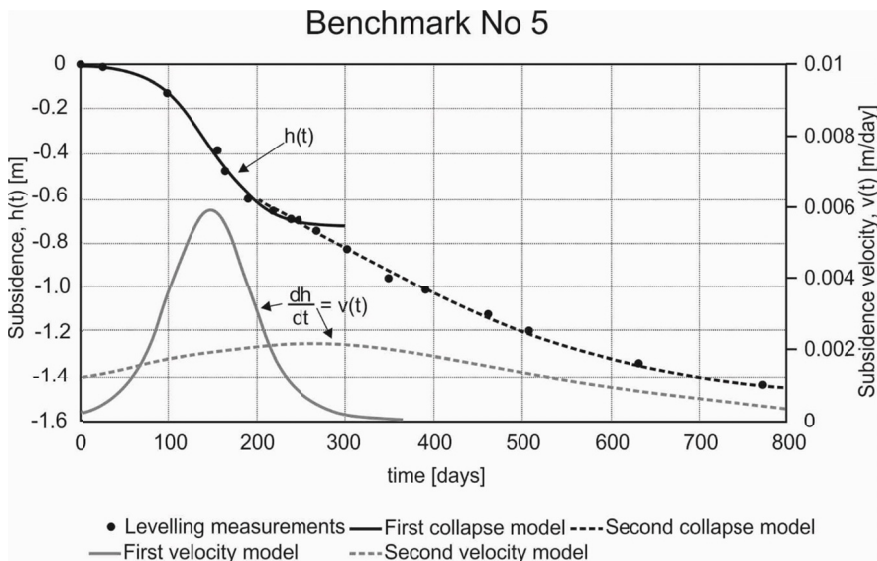


Fig. 3. The results of geodetic measurements – subsidence and subsidence velocity against time

4.2. Interpretation of seismic data

The two seismic methods using the obtained seismic traces allowed us to independently determine the P- and S-wave velocities. Refracted P-arrivals were used to calculate P-wave velocity in ductile and brittle layers and MASW interpretation was used to calculate the S-wave velocities. The results for both of the near-surface layers were presented in Figures 4a and 5a. Distinguished variations of the velocity of P- and S-waves for a ductile layer are present slightly after the occurrence of the maximum subsidence velocity. The velocity increase could be related to the appearance of compression forces for 0° direction (accordingly to exploitation direction). After this period, rapid changes in velocities were observed. Finally, the velocity of P- and S- waves became more stable.

Changes in directions of maximum P- and S-wave velocities were observed during subsidence development. The rotation of the velocity vector is probably related to the changes in time stress regime that is visible in Fig. 4a and 5a (circles). The spatial changes in velocities indicate that the maximum velocity of P-waves is perpendicular to S-wave maxima. The maximum P-wave velocity directions are in accordance with the direction of the longwall exploitation. In addition, the velocity spatial changes show a relative increase in velocity in all directions at a time that corresponds to the final stage of subsidence trough development. An inverse relation is observed for P-wave velocity in the brittle layer (Fig. 5a – circles). In this case, the significant velocity drop is observed for the direction parallel to the exploitation direction. It is assumed that in the brittle layer, due to development of the subsidence trough, the system of newly produced fractures is perpendicular to the exploitation direction. The presence of new fractures results in the relevant velocity decrease.

Similar effects are observed for time- and space-dependent changes in shear modulus (Figs 4b and 5b). Moreover, it is confirmed by high absolute values of the attenuation coefficient, which can

be considered a result of disturbance in the brittle layer (Fig. 6). Nevertheless, the determination of attenuation coefficient is more uncertain than the velocity calculation. In addition, a velocity increase-attenuation decrease is observed.

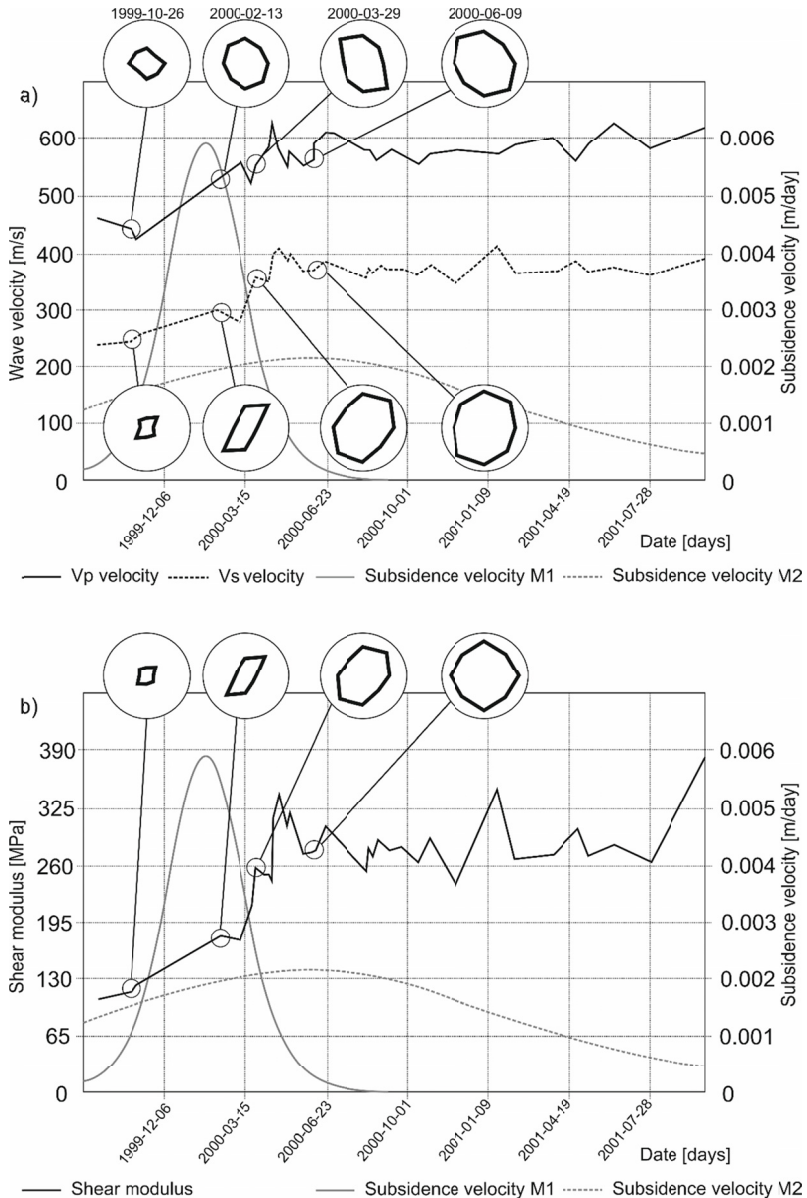


Fig. 4. Temporal changes in the seismic wave velocity (a) and shear modulus (b) in the ductile layer for 0° direction on the rosette compared to subsidence velocities in two stages M1 and M2. In circles the spatial changes of the parameters were shown for four selected dates: 1999-10-26, 2000-02-13, 2000-03-29, 2000-06-09, respectively. The size of rosettes in the rows are normalized according to the first one

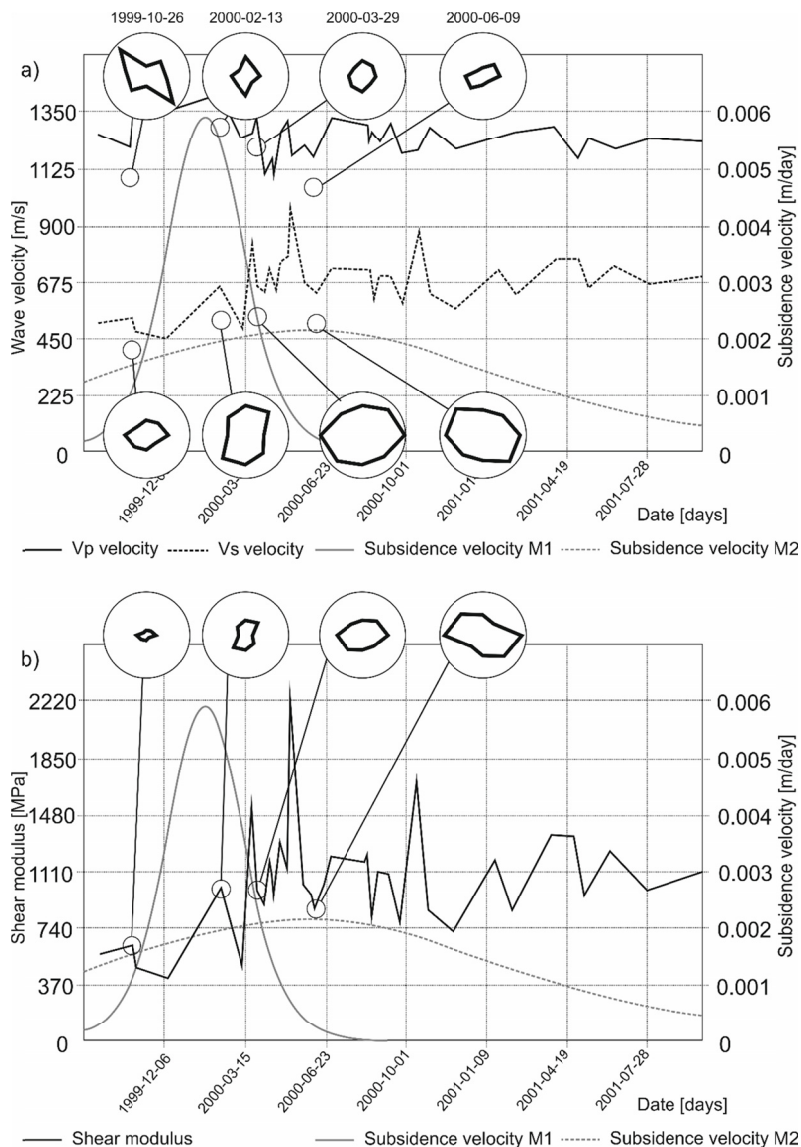


Fig. 5. Temporal changes in the seismic wave velocity (a) and shear modulus (b) in the brittle layer for 0° direction on the rosette compared to subsidence velocities in two stages M1 and M2. In circles the spatial changes of the parameters were shown for four selected dates: 1999-10-26, 2000-02-13, 2000-03-29, 2000-06-09, respectively. The size of rosettes in the rows are normalized according to the first one

5. Discussion and conclusions

The data analysis of the old and new seismic approaches indicated similar results. The velocity values of body waves and attenuation coefficients for brittle and ductile layers agreed with

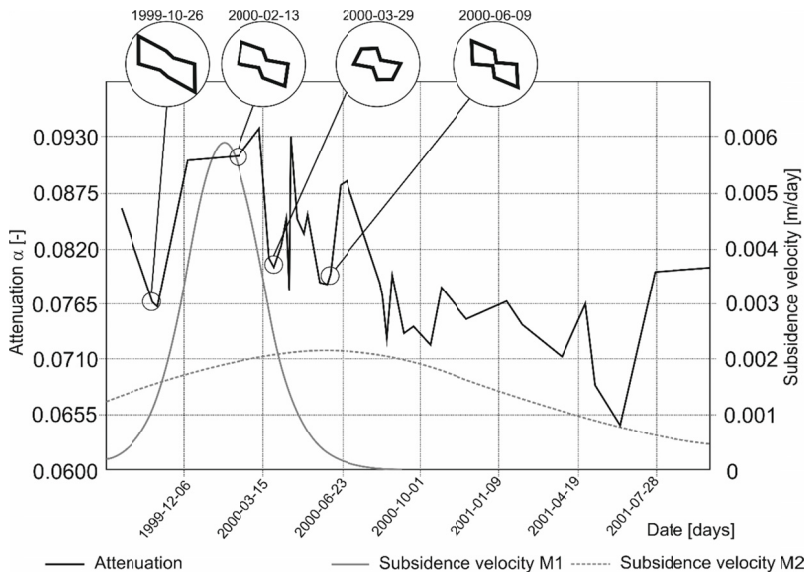


Fig. 6. Temporal changes in the attenuation coefficient in the brittle layer for 0° direction on the rosette compared to subsidence velocities in two stages M1 and M2. In circles the spatial changes of the parameter were shown for four chosen dates: 1999-10-26, 2000-02-13, 2000-03-29, 2000-06-09, respectively. The size of rosettes in the rows are normalized according to the first one

those presented in other studies (Gustkiewicz et al., 1988, 2002; Jochymczyk, 2005; Kovačević et al., 2013). The high values of attenuation coefficients show that the geologic environment is strongly disturbed. Rapid and sharp changes in seismic parameters indicate that subsidence development was not fluent. This phenomenon was interpreted as blocky deformation of the brittle medium.

The stabilization of seismic parameters after subsidence development suggests that after subsidence deformation any new cracks and disturbance are not observed. Similar conclusions were presented by Doležalová et al. (2009). The last stage of subsidence is characterized by a reduction of increments of subsidence, surface stabilization, and disturbed overlaying rocks dislocated to the extracted deposit and pressed down to the original amount or transformed into a new amount, which corresponds to the balanced condition. This stage takes several years, depending on the strength of accompanying rocks (Doležalová et al., 2009).

1. During the process of subsidence trough development in the subsurface rock cover, one may observe two characteristic periods with very rapid changes of body wave velocities and attenuation coefficients. Those changes appeared near the surface 3 months after underground exploitation.
2. Observed variations of the seismic parameters significantly correlate with increased velocity of the surface subsidence.
3. Generally, after completion of exploitation the values of recorded seismic parameters returned to the balanced condition. The observed variation could be produced by changes of ground water regime as well as the effect of the parameter calculation uncertainties caused by an observational error or propagation of uncertainty.

Levelling and seismic observations confirm the existence of a very variable state of stress regime in the near surface rock mass in accordance with the process of subsidence trough development.

References

- Bamford D., Nunn K.R., 1979. *In Situ Seismic Measurements of Crack Anisotropy in the Carboniferous Limestone of Northwest England*. Geophysical Prospecting 27 (2), 322-338. doi: 10.1111/j.1365-2478.1979.tb00973.x.
- Belfer I., Bruner I., Keydar S., Kravtsov A., Landa E., 1998. *Detection of shallow objects using refracted and diffracted seismic waves*. Journal of Applied Geophysics 38 (3), 155-168.
- Blachowski J., Cacon S., Milczarek W., 2009. *Analysis of post-mining ground deformations caused by underground coal extraction in complicated geological conditions*. Acta Geodyn. Geomater 6, 351-357.
- Bogusz M., Mendecki M., 2011. *Seismic and Geodetic Observations of Subsidence Trough Development Over a Longwall Face in a Coal Bed Under Extraction Geophysics*. Idziak A.F, Dubiel R. (Eds). *Mining and Environmental Protection*. Springer, Berlin, 71-79. doi: 10.1007/978-3-642-19097-1_7.
- Carvalho J., Lisboa J.V., Torres L., Mendes-Victor L.A., 2000. *Rock mass evaluation using in-situ velocity and attenuation measurements*. European Journal Of Environmental And Engineering Geophysics 5, 15-31.
- Carvalho J., Torres L., Castro R., Dias R., Mendes-Victor L., 2009. *Seismic velocities and geotechnical data applied to the soil microzonation of western Algarve, Portugal*. Journal of Applied Geophysics 68 (2), 249-258. doi: 10.1016/j.jappgeo.2009.01.001.
- Crampin S., McGonigle R., Bamford D., 1980. *Estimating crack parameters from observations of P-wave velocity anisotropy*. Geophysics 45 (3), 345-360.
- Dal Moro G., Moura R.M.M., Moustafa S.S., 2015a. *Multi-component Joint Analysis of Surface Waves*. Journal of Applied Geophysics 119, 128-138. doi: 10.1016/j.jappgeo.2015.05.014.
- Dal Moro G., Pipan M., Gabrielli P., 2007. *Rayleigh wave dispersion curve inversion via genetic algorithms and marginal posterior probability density estimation*. Journal of Applied Geophysics 61, 39-55. doi: 10.1016/j.jappgeo.2006.04.002.
- Dal Moro G., Ponta R., Mauro R., 2015b. *Unconventional optimized surface wave acquisition and analysis: Comparative tests in a perilagoon area*. Journal of Applied Geophysics 114, 158-167. doi: 10.1016/j.jappgeo.2014.12.016.
- Doležalová H., Kajzar V., Souček K., Staš L., 2009. *Evaluation of mining subsidence using GPS data*. Acta Geodyn Geomater 6, 359-367.
- Doležalová H., Kajzar V., Souček K., Staš L., 2012. *Analysis of surface movements from undermining in time*. Acta Geodyn. Geomater 9, 389-400.
- Foti S., Lai C.G., Rix G.J., Strobbia C., 2014. *Surface wave methods for near-surface site characterization*. CRC Press.
- Gustkiewicz J., Zuberek W.M., Jochymczyk K., Kaczor D., 2002. *Geophysical monitoring of soil deformation due to underground mining*. Ogasawara H., Yanagidani T., Ando M. (Eds) *Seismogenic Process Monitoring*, AA Balkema Publishers, 25-36.
- Ismail A., Denny F.B., Metwaly M., 2014. *Comparing continuous profiles from MASW and shear-wave reflection seismic methods*. Journal of Applied Geophysics 105, 67-77. doi: 10.1016/j.jappgeo.2014.03.007.
- Jochymczyk K., 2005. *Levelling and seismic refraction measurements of ground subsidence in a mining area*. Acta Geodyn. Geomater 2, 151-157.
- Kadlečík P., Kajzar V., Nekvasilová Z., Wegmüller U., Doležalová H., 2015. *Evaluation of the subsidence based on dInSAR and GPS measurements near Karvina, Czech Republic*. AUC Geographica 50 (1), 51-61. doi: 0.14712/23361980.2015.86.
- Kadlečík P., Schenk V., Seidlova Z., Schenkova Z., 2010. *Analysis of vertical movements detected by radar interferometry in urban areas*. Acta Geodyn. Geomater 7, 371-380.
- Kajzar V., Doležalová H., 2013. *Monitoring and Analysis of Surface Changes from Undermining*. GeoScience Engineering 59 (4), 1-10. doi: 10.2478/gse-2014-0062.

- Karakostas V., Mirek K., Mesimeri M., Papadimitriou E., Mirek J., 2017. *The Aftershock Sequence of the 2008 Achaia, Greece, Earthquake: Joint Analysis of Seismicity Relocation and Persistent Scatterers Interferometry*. *Pure and Applied Geophysics* 174, 151-176. doi: 10.1007/s00024-016-1368-y.
- Knothe S., 1980. *Influence of time on the course of displacement, deformation of the rock mass and land surface caused by mining exploitation*. Borecki M. (Ed.) *Surface protection against mining damage*, Wydawnictwo "Śląsk" Katowice (in Polish).
- Knothe S., 1984. *Predicting the impacts of mining exploitation*. Wydawnictwo "Śląsk" Katowice (in Polish).
- Kochmański T., 1980. *Tadeusz Kochmański Theory*. Borecki M (Ed.) *Surface protection against mining damage*, Wydawnictwo "Śląsk" Katowice (in Polish).
- Lin C.P., Chang C.C., Chang T.S., 2004. *The use of MASW method in the assessment of soil liquefaction potential*. *Soil Dynamics and Earthquake Engineering* 24 (9), 689-698. doi: 10.1016/j.soildyn.2004.06.012.
- Mirek K., Mirek J., 2016. *Observation of underground exploitation influence on a surface in Budryk, Sośnica, and Makoszowy coal mine area*. *Polish Journal of Environmental Studies* 25 (5A), 57-61.
- Park C.B., Miller R.D., Xia J., 1999. *Multichannel analysis of surface waves*. *Geophysics* 64(3), 800-808.
- Schön J.H., 1996. *Physical Properties of Rocks: fundamentals and principles of Petrophysics*. Pergamon Press, Oxford.
- Sloan S.D., Nolan J.J., Broadfoot S.W., McKenna J.R., Metheny O.M., 2013. *Using near-surface seismic refraction tomography and multichannel analysis of surface waves to detect shallow tunnels: A feasibility study*. *Journal of Applied Geophysics* 99, 60-65. doi: 10.1016/j.jappgeo.2013.10.004.
- Stan-Kleczek I., Mendecki M.J., 2014. *The use of active seismic methods to study seismic waves anisotropy in Triassic dolomites*. Alejano R, Perucho A, Olalla C, Jiménez R (Eds) *Rock Engineering and Rock Mechanics: Structures in and on Rock Masses*. Taylor & Francis Group, London, 1213-1217.
- Stan-Kleczek I., Mendecki M.J., 2016. *Application of Multichannel Analysis of Surface Waves to S-Phase Wave Anisotropy Estimation*. *Acta Geophysica* 64 (5), 1593-1604. doi: 10.1515/acgeo-2016-0058.
- Turesson A., 2007. *A comparison of methods for the analysis of compressional, shear, and surface wave seismic data, and determination of the shear modulus*. *Journal of Applied Geophysics* 61 (2), 83-91. doi: 10.1016/j.jappgeo.2006.04.005.
- Xu C., Butt S.D., 2006. *Evaluation of MASW techniques to image steeply dipping cavities in laterally inhomogeneous terrain*. *Journal of Applied Geophysics* 59 (2), 106-116. doi: 10.1016/j.jappgeo.